ASM Sc. J., 14, Special Issue 1, 2021 for ICSTSS2018, 63-69

Improved Capacitive Performance of Activated Carbon-doped Titanium Dioxide for Supercapacitor Electrode Material

Nurul Infaza Talalah Ramli[1*], Hartini Ahmad Rafaie[1], Mohd Firdaus Kasim[2] and Mohd Syafiq Affandi Mohd Rusdi[1]

[1]*Faculty of Applied Sciences, Universiti Teknologi MARA Pahang, Bandar Tun Abdul Razak Jengka, Pahang, Malaysia*
[2]*Centre for Nanomaterials Research, Institute of Science, Universiti Teknologi MARA, Shah Alam, Selangor, Malaysia*

The preparation and supercapacitive performance of Incorporated Titanium Dioxide (TiO_2) – activated carbon (AC) were studied in this work. The crystalline phase and the presence of desired functional group were revealed through X-ray diffraction and Fourier Transform Infra-red analysis, respectively. The supercapacitive behaviours of the prepared samples were analysed via cyclic voltammetry (CV) analysis by means of three-electrode system. CV analysis display a remarkable specific capacitance (C_s) value of 267 Fg^{-1} at 50 mVs^{-1}, by incorporating 20 wt% of TiO_2 into the AC matrices. With the combined contribution from high conductivity AC and transition metal oxide, the C_s value has been found to increase substantially with respect to AC electrode. Moreover, the addition of 20 wt% TiO_2 enhanced the electrochemical stability with 90% capacity retention after 100th consecutive cycles. A notable supercapacitive performance shown by the sample is ascribed to the synergistic effect of electric double layer capacitance and pseudocapacitance produced by the combined matrices.

Keywords: activated carbon; electrochemical; energy storage; supercapacitor; titanium oxide

I. INTRODUCTION

The energy storage system has been used in diverse applications like portable electronics, military equipment and hybrid electric vehicle with various energy storage requirement. The mounting importance of energy has led to the extensive efforts of finding materials that have both superior energy storage properties: high power and energy density (Li *et al.*, 2008). Supercapacitors are one of the leading energy storage device available to date. Supercapacitors are constructed with high capacitance which has attracted prominent attention due to their potential applications in electronic devices (Wang *et al.*, 2005). The ability in combining the benefit of the conventional capacitors that possess high power density with the high energy density of rechargeable batteries make supercapacitors a popular protocol of energy storage device. In recent years, increasing demand for energy storage and consumption has triggered the findings of efficient energy storage capabilities in every domain (Sakamoto, 2002). Hence, much interest in finding materials that has the ability to store energy has arised due to this current energy crisis. Presently, activated carbon (AC) is noted to be one of the materials used for energy storage purposes (Khiew *et al.*, 2013). The advantage of having high specific surface area (SSA) has brought AC to notability. Therefore, SSA allows a greater number of electrochemical reaction sites which enable more electron transfer to the charged collector simultaneously. However, the performance of AC as a singular material matrix is relatively poor in terms of its specific capacitance and specific energy (Chen *et al.*, 2016). Hence, in order to refine the energy storage capability of carbon-based material, the addition of pseudocapacitance- type material such as transition metal oxide (TMO) is of prime importance. TMO is proven to be vital in enhancing the storage properties of carbon-based material due to its rapid ion insertion and extraction within

---

*Corresponding author's e-mail: nurulinfaza@uitm.edu.my

the material (Sakamoto, 2002). This will then overcome the limitation of slow diffusion and volumetric strain in the energy storage material (Kim *et al.*, 2013). Studies have reported the reliability of incorporated TMO such as zinc oxide (ZnO), iron oxide (Fe_3O_4) and ruthenium oxide (RuO_2) in carbon-based material (Li *et. al.*, 2013; Qi *et. al.*, 2013; Ramli *et al.*, 2017). In this specific study, titanium dioxide (TiO_2) is chosen prior to its synthesis easiness and high specific energy properties. This study will emphasise on the effect of TiO_2 addition on the overall electrochemical energy storage performance of AC. The escalation in specific capacitance of the AC/TiO_2 composites can be ascribed to the synergistic effect of high surface area AC and high specific energy TiO_2. It is believed that the enhancement in specific capacitance is due to the development of conductive network in the composites material when the contact between carbon and transition metal oxides material occurs. Hence in this study, incorporation of both carbon based and metal oxides materials via ultasonic-assisted sol-gel method is proposed in order to improve the overall supercapacitive behaviour.

II. MATERIALS AND METHOD

A. Materials

All the chemical reagents used including titanium dioxide (TiO_2) powder, activated carbon (AC), and sulphuric acid (H_2SO_4) were analytically pure and purchased from Sigma-Aldrich. Deionised (DI) water were also used throughout the experiment.

B. Preparation of Activated Carbon Doped TiO_2

The AC doped with TiO_2 nanoparticles were synthesised via chemical mixing and stirring at different weight ratios of AC and TiO_2. The weight ratios ranging from 5 %, 10 %, 20 %, 30 % and 40 % of TiO_2 addition to the AC samples were thoroughly prepared. The samples are labelled as ACTi$O_2$5, ACTi$O_2$10, ACTi$O_2$20, ACTi$O_2$30 and ACTi$O_2$40, accordingly. A certain amount of AC and purified TiO_2 were dissolved into 100 mL of DI water and sonicated for one hour to achieve a stable suspension. The sonication process were followed by 2 hours of stirring by using magnetic stirrer. Then, the sample were dried in a conventional oven at 40 °C for 24 hours to obtain a powdery samples.

C. Characterizations

The samples undergo a certain characterisation process in order to evaluate its physicochemical and electrochemical properties. The physicochemical properties were assessed via X-Ray Diffraction (XRD) analysis using PANalytical model (Cu Kα radiation, λ= 0.154 nm) at room temperature, and Fourier transform infrared (FTIR) using Nicolet 6700 FTIR machine. Meanwhile, the electrochemical analysis was evaluated via cyclic voltammetry (CV) analysis using potentiostat Metrohm (AUTOLAB PGSTAT 204), with a standard three electrodes cell configuration. In this cell system, the prepared samples were drop-casted on the working electrode (glassy carbon), while Ag/AgCl served as the reference electrode and platinum wire as counter electrode.

III. RESULTS AND DISCUSSION

A. Physicochemical properties

XRD analysis was performed in order to evaluate the crystallographic information of the AC and AC/TiO_2 composite samples. Figure 1 shows the typical XRD spectra of pure AC, pure TiO_2, and AC/TiO_2 at various weight ratios in the range of 20-80°. A broad peak approximately at 2θ = 27° was assigned to the amorphous carbon phase. Diffraction peaks which correspond to A (101), R (110), R (101), A (112), R (111), R (210), A (200), A (105), R (211), A (211), R (220), A (118), A (220), R (301) and A (215) planes were in accordance to the formation of mixed phase of TiO_2 (anatase (JCPDS 21-1272) and rutile (JCPDS 21-1276)). Moreover, the absence of impurity peaks indicates high degree of purity (Filippo *et al.*, 2015). An increasing trend of peak intensity can be seen as the TiO_2 content was increased in the sample. On the contrary, the formation of amorphous phase of carbon was gradually disappeared as the amount of TiO_2 increases. The XRD spectra of pure AC, pure TiO_2 and ACTiO_2 ranges from 24-27° is presented in Figure 2. A slight peak shift can be seen on the major peak A (101). As the amount of TiO_2 increased in the sample, the peak shifted slightly to the left. This might be due to the radius ratio of C^{4+} (0.16 Å) and Ti^{4+} (0.61 Å). Furthermore, these shifting trend might cause by the disorder in the crystal lattice and rising distortion of the TiO_2 crystal structure during the access of carbon ions into TiO$_2$ crystal lattice (Fan *et al.*, 2017).

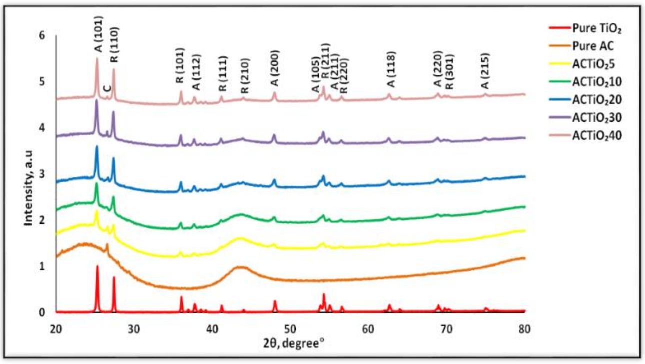

Figure 1. XRD pattern of pure AC, pure TiO$_2$ and ACTiO$_2$ samples in the range 20 – 80°

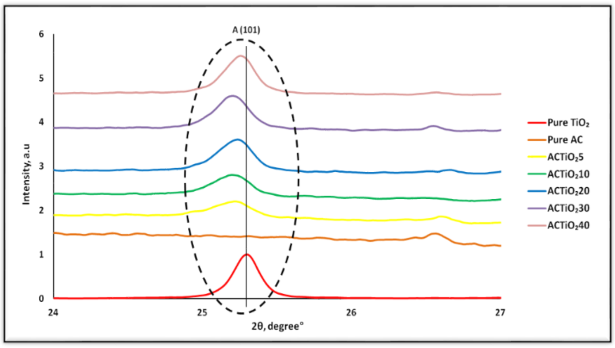

Figure 2. XRD pattern of pure AC, pure TiO$_2$ and ACTiO$_2$ samples in the range 24 – 27°

The crystallite size of the samples were estimated by using the Debye-Scherrer's equations as shown in Equation (1), which expresses as:

$$D_f = \frac{k\lambda}{\beta \cos\theta} \tag{1}$$

where D_f is the Crystalline size (in nm), k is equal to 0.94, λ is the wavelength of the incident X-ray which set to be 1.54060 Å, β is the full width at half maximum (FWHM) of the diffraction peak (after removal of the instrumental broadening) and 2θ is the diffraction angle.

The crystallite size of pure TiO$_2$ and ACTiO$_2$ at different weight ratios was found to be in the range of 28.34 to 45.47 nm, respectively. Table 1 provides the crystallite size data for pure TiO$_2$ and ACTiO$_2$ composites at various weight ratios. An increasing trend of crystallite size were observed as an increased of TiO$_2$ amount were added to the pure AC sample. This was due to the size ratio of pure TiO$_2$ and AC, where TiO$_2$ were evidently larger than AC particle.

Table 1. Average crystallite size of pure TiO$_2$ and ACTiO$_2$ at different weight ratios

Sample	**2θ**	**FWHM, β (degree)**	**Average crystallite size, D_f (nm)**
Pure TiO$_2$	25.269	0.187	45.472
ACTiO$_2$5	25.200	0.300	28.340
ACTiO$_2$10	25.167	0.270	31.487
ACTiO$_2$20	25.194	0.263	32.327
ACTiO$_2$30	25.172	0.249	34.143
ACTiO$_2$40	25.222	0.228	37.292

FTIR studies have been performed in the range of 500 to 4000 cm^{-1} frequency range as presented in Figure 3. From Figure 3, the FTIR spectrums of the pure AC shows peaks between 1700–1500, 1300–900 and 600 – 500 cm^{-1}. The band at about 1564 cm^{-1} is ascribable to C=C bonds of the aromatic ring compound type. Meanwhile, the band appearing at 1240 cm^{-1} is caused by C-O vibrations. The adsorption at 548 and 575 cm^{-1} are assigned to the C-H vibrations. Besides, this characteristics absorption band attributed to plane deformation mode of C-H for dissimilar substituted benzene ring (Benadjemia *et al.,* 2011). In the spectrum of pure TiO$_2$, the peaks appeared between 1800–1700, 1400–1100 and 900-500 cm^{-1}. The carbonyl bond (C=O) appear from the free ester at 1739 cm^{-1} (Doloksaribu *et al.,* 2017). In addition, the peak at 1216 and 1365 cm^{-1} of pure TiO$_2$ can arise from C–O vibrations. The band at 560 and 713 cm^{-1} could be assigned to the bending vibration of O-Ti-O bond in the TiO$_2$ lattice. Furthermore, the FTIR spectrum obtained for the ACTiO$_2$20 sample has spectral range between 3800–3400, 1800–1700, 1600–1500, 1400–1100 and 600-500 cm^{-1}. In the high wave number spectral range, a band at 3740 cm^{-1} can be assigned to hydrogen bond (O–H) in phenolic groups. Apart from that, the presence of additional new peak can be observed at 1542 cm^{-1} that indicates the C=C bonds of the aromatic ring compound type. Moreover, the peak at 553 and 578 cm^{-1} in the spectra of ACTiO$_2$20 was the O–Ti–O bond that belonged to the characteristic absorption peaks of pure TiO$_2$

that bind at the surface of AC and further showing the successful loading of TiO_2 on AC (Burgos & Langlet, 1999). It was found that FTIR analysis revealed the presence of various characteristic functional groups in $ACTiO_2$ sample. As indicated by Simon and Gogotsi (2010), oxygen functional groups have a great influence on the electrochemical properties of carbon materials. Li *et al.* (2011) also stated that, the carbonyl and carboxyl groups are beneficial to pseudocapacitance generated from fast faradic reactions that can contribute to the capacitance of electrode. Therefore, the $ACTiO_2$20 sample evidently has good capacitance and AC-TiO_2 composite can be used effectively as supercapacitor electrode material.

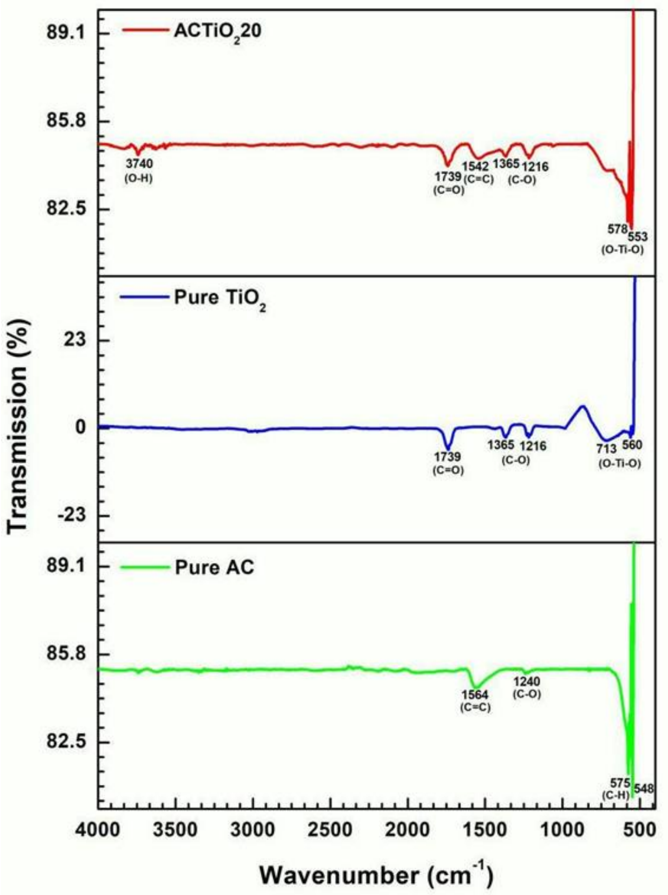

Figure 3. FTIR spectra of pure AC, pure TiO_2 and $ACTiO_2$ samples

B. Electrochemical Properties

Figure 4 shows the CV curves of AC/TiO_2 nanoparticles within the potential range from -0.2 to 0.8 V at 50 mVs^{-1} and 100 mVs^{-1} scan rates. As studied by Khiew *et al.* (2013), a massive contribution of pseudocapacitance to the system is believed to form the perfect rectangular voltammograms from the aberration of the samples. The adjacent of ideal parallelogram shape can be seen from the CV curve, which indicates less but appropriate contribution from redox reaction. When the TiO_2 content was increased up to 20 wt %, an enhanced specific capacitance value was observed. Nevertheless, addition in weight percentage of more than 20 wt % of TiO_2 will decrease the capacitive value, as demonstrated in Figure 4. The capacitance value degradation was considerably affected by the weight ratio of TiO_2 to the AC particles. Overall, it may be said combining the carbon element with metal oxide obviously improved the charge storage capability of the composite.

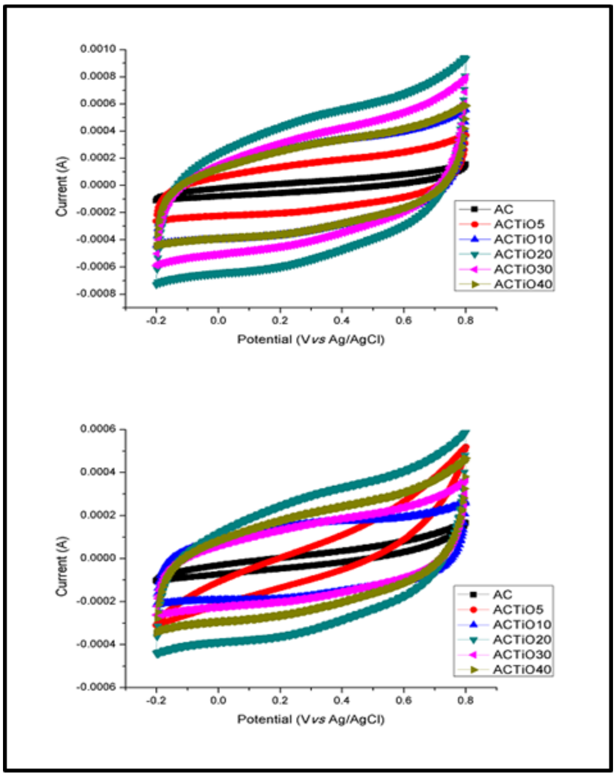

Figure 4. CV curves of various weight ratios AC/TiO_2 at 50 mVs^{-1} (above) and 100 mVs^{-1} (below)

It can be observed that the specific capacitances of all samples are decreased steadily when the scan rates increased. This trend was due to the chemical adsorption/desorption or redox reaction that takes place on the surfaces of the electrodes, enabling electrolyte ions to relocate into the inner pores of the electrodes at lower scan rates (Chen *et al.*, 2016). On the contrary, at higher scan rates, the electrolyte ions have insufficient time to accumulate on the electrode surface. For this reason, the lower scan rate exhibits a better specific capacitance for energy storage devices. The supercapacitor performance at 50 mVs^{-1} and 100 mVs^{-1} scan rates are presented in Figure 5. The bare activated carbon electrode exhibit specific capacitance of 22.128 Fg^{-1} and 14.819 Fg^{-1} at 50 mVs^{-1} and 100 mVs^{-1} respectively. By referring to the Figure 5, the specific capacitance of AC/TiO$_2$ was higher than the activated carbon alone at both 50 mVs^{-1} and 100 mVs^{-1} scan rates. These properties enhancement is caused by the adequate amount of available sites for electrochemical reactions occurrence. Higher conductivity and synergistic behaviour of the combined materials were another contributing factors that leads to the improved supercapacitor performance (Ramli *et al.*, 2017). AC/TiO$_2$20 exhibits the highest capacitive value with 267.910 Fg^{-1} Cs value at 50 mVs^{-1}. Similar trend has been observed for other ratio of AC/TiO$_2$ when the scan rate was increased from 50 to 100 mVs^{-1}. Apart from that, ACTiO$_2$20 shows highest specific capacitance with 267.910 Fg^{-1} and 226.190 Fg^{-1} at 50 mVs^{-1} and 100 mVs^{-1}, respectively. Thus, there was an optimum value observed from the CV trend. Decreasing trend in Cs values was spotted as the amount of TiO$_2$ increased from 30% to 40 % wt. This is due to sample agglomeration which caused by excessive TiO$_2$ loading *(Qi et al.*, 2013). According to Li *et al.* (2013), the agglomeration of TiO$_2$ will diminish the storage capacity as it engenders blockage and restrict the access of electrolyte in the composite. Consequently, in order to conserve great conductivity and easy ion migration supplied by the carbon material, the TiO$_2$ content should not surpass the percentage of ACTiO$_2$20.

The cyclic stability of ACTiO$_2$20 sample was determined through CV test for 100 cycles at a scan rate of 100 mVs^{-1}. Figure 6 shows the cyclic stability of ACTiO$_2$20. The Cs values of ACTiO$_2$20 remain approximately the same as its initial values.

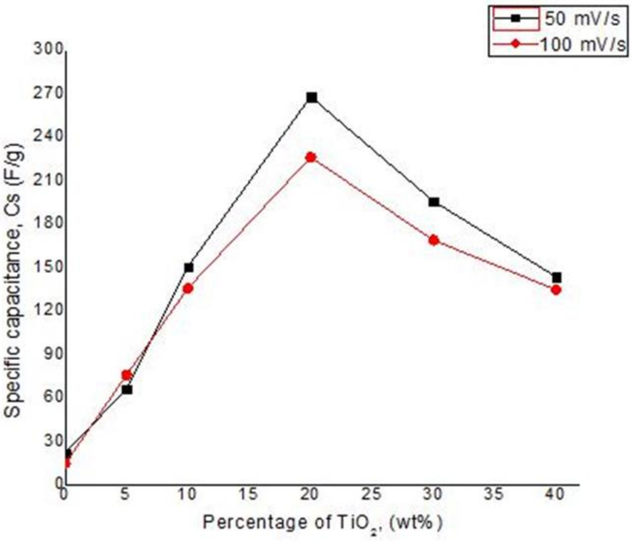

Figure 5. Supercapacitor performance at 50 and 100 mV/s

As shown in Figure 6, the respective CV curves retained their rectangular voltammograms shapes throughout the complete cycling test. Moreover, it was observed that ACTiO$_2$20 retained 90% of its initial specific capacitance after 100 respective cycles, which demonstrates excellent electrochemical stability during cycling life and evidently implies its prospective practical usage in diverse applications. High-conductivity of ACTiO$_2$ averts the capacity loss and contributes towards the outstanding stability of ACTiO$_2$20.

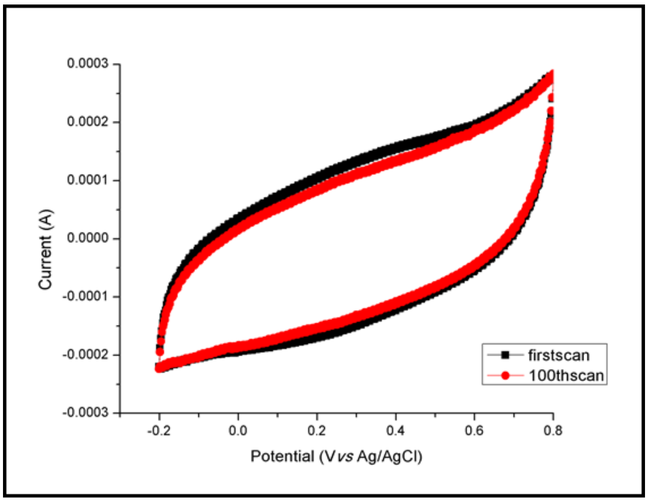

Figure 6. CV curves of ACTiO$_2$20 at 1st and 100th cycles

IV. CONCLUSION

The AC doped TiO$_2$ nanocomparticles have been prepared successfully via ultrasonic assited sol-gel method. Of 5 different weight ratios samples prepared, the sample at 20 wt% of TiO_2 addition shows an optimal supercapacitive behavior. An in depth electrochemical study shows that $ACTiO_2$20 exhibits good electrochemical capacitance performance with the specific capacitance value of 267.91 and 226.19 Fg^{-1} at scan rates of 50 and 100 mvs^{-1}, respectively. Remarkably, $ACTiO_2$20 also display great electrochemical stability performance. Besides, XRD pattern reveal that pure AC, pure TiO_2 and $ACTiO_2$ samples were pure in phase. On the other note, the same analysis shows an increment in crystalline size as TiO_2 were doped into the AC, in comparison to pure TiO2. Smaller crystallite size of $ACTiO_2$20 composite is attributed to a greater active surface area that enhance the electrochemical stability. Moreover, the presence of various characteristic functional groups in $ACTiO_2$20 sample was revealed by the FTIR analysis. The carbonyl group (C=O) found in hybrid nanocomposite samples contribute the most to the pseudocapacitance through faradic reaction. Due to its outstanding electrochemical and physicochemical characterisation, $ACTiO_2$ composite can be a promising candidate for next generation high performance electrochemical supercapacitor electrode material.

V. ACKNOWLEDGEMENT

The authors acknowledge the financial support from Malaysian Government and University Teknologi MARA Pahang, and would like to express lots of gratitude to the Centre of Nanomaterials, Institutes of Science University Teknologi MARA Shah Alam for their characterisation equipment.

VI. REFERENCES

Benadjemia, M, Millière, L, Reinert, L, Benderdouche, N & Duclaux, L 2011, 'Preparation, characterisation and Methylene Blue adsorption of phosphoric acid activated carbons from globe artichoke leaves', Fuel Processing Technology, vol. 92, no. 6, pp. 1203–1212.

Burgos, M & Langlet, M 1999, 'Condensation and densification mechanism of sol-gel TiO2 layers at low temperature', Journal of Sol-Gel Science and Technology, vol. 16, no. 3, pp. 267–276.

Chen, Y-C, Wen, C-Y, Wang, C-M, Ho, C-W, Lin, S-Y & Chen, Y-L 2016, 'Characterization of transition-metal oxide deposition on carbon electrodes of a supercapacitor', Applied Sciences, vol. 6, no. 12, pp. 413.

Doloksaribu, M, Harsojo, Triyana, K & Prihandoko, B 2017, 'The effect of concentration nanoparticles MnO_2 doped in activated carbon as supercapacitor electrodes', International Journal of Applied Engineering Research, vol. 12, no. 19, pp. 8625–8631.

Fan, H, Zhang, H, Luo, X, Liao, M, Zhu, X, Ma, J & Song, Y 2017, 'Hydrothermal solid-gas route to TiO2 nanoparticles/nanotube arrays for high-performance supercapacitors', Journal of Power Sources, vol. 357, pp. 230–240.

Filippo, E, Carlucci, C, Capodilupo, AL, Perulli, P, Conciauro, F, Corrente, GA, Gigli, G 2015, 'Enhanced photocatalytic activity of pure anatase Tio_2 and Pt-Tio_2 nanoparticles synthesised by green microwave assisted route 2', Experimental Section Materials Research, vol. 18, no. 3, pp. 473–481.

Sakamoto, JS 2002, 'Studies of ion electroadsorption in supercapacitor electrodes', Journal of the Electrochemical Society, vol. 149, no. 1, pp. A26–A30.

Khiew, P, Ho, M, Chiu, W, Shamsudin, R, Azmi, M, & Chia, C 2013, 'Synthesis and electrochemical characterisation of iron oxide / activated carbon composite electrode for symmetrical supercapacitor', International Journal of Chemical, Molecular, Nuclear, Materials and Metallurgical Engineering, vol. 7, no. 8, pp. 615–619.

Kim, H, Cho, M, Kim, M, Park, K, Gwon, H, Lee, Y & Roh, KC 2013, 'A novel high energy hybrid supercapacitor with an anatase TiO_2 – reduced graphene oxide anode and an activated carbon cathode', Advanced Energy Materials, vol. 3, no. 11, pp. 1500-1506.

Li, LX & Li, F 2011, 'The effect of carbonyl, carboxyl and hydroxyl groups on the capacitance of carbon nanotubes', New Carbon Materials, vol. 26, no. 3, pp. 224–228.

Li, Z, Jin-yan, S, Ji-yan, Z & Ning, W 2008, 'High voltage super-capacitors for energy storage devices applications', vol. 1, pp. 8–11.

Li, Z, Zhou, Z, Yun, G, Shi, K, Lv, X & Yang, B 2013, 'High-performance solid-state supercapacitors based on graphene-ZnO hybrid nanocomposites', Nanoscale Research Letters, vol. 8, no. 1, pp. 1–9.

Qi, T, Jiang, J, Chen, H, Wan, H, Miao, L & Zhang, L 2013, 'Synergistic effect of Fe_3O_4/reduced graphene oxide nanocomposites for supercapacitors with good cycling life', Electrochimica Acta, vol. 114, pp. 674–680.

Ramli, NIT, Rashid, SA, Mamat, MS, Sulaiman, Y, Zobir, SA & Krishnan, S 2017, 'Incorporation of zinc oxide into carbon nanotube/graphite nanofiber as high performance supercapacitor electrode', Electrochimica Acta, vol. 228, pp. 259–267.

Simon, P & Gogotsi, Y 2010, 'Charge storage mechanism in nonporous carbons and its consequence for electrical double layer capacitors', Philosophical Transactions Series A, Mathematical, Physical, and Engineering Sciences, vol. 368, pp. 3457–3467.

Wang, YG, Wang, ZD & Xia, YY 2005, 'An asymmetric supercapacitor using RuO_2/TiO_2 nanotube composite and activated carbon electrodes', Electrochimica Acta, vol. 50, no. 28, pp. 5641–5646.